

Quantification of Macular Microvascular Changes in Patients With Retinitis Pigmentosa Using Optical Coherence Tomography Angiography

Daiki Inooka, Shinji Ueno, Taro Kominami, Akira Sayo, Satoshi Okado, Yasuki Ito, and Hiroko Terasaki

Department of Ophthalmology, Nagoya University Graduate School of Medicine, Nagoya, Japan

Correspondence: Shinji Ueno, Department of Ophthalmology, Nagoya University Graduate School of Medicine, 65 Tsuruma-cho, Showa-ku, Nagoya 466-8550, Japan; ueno@med.nagoya-u.ac.jp.

Submitted: October 24, 2017
Accepted: December 18, 2017

Citation: Inooka D, Ueno S, Kominami T, et al. Quantification of macular microvascular changes in patients with retinitis pigmentosa using optical coherence tomography angiography. *Invest Ophthalmol Vis Sci*. 2018;59:433–438. <https://doi.org/10.1167/iovs.17-23202>

PURPOSE. To evaluate the microvascular changes in eyes with RP quantitatively using optical coherence tomography angiography (OCTA) and to determine whether the correlations between these indices and the severity of RP are significant.

METHODS. This was a retrospective, observational study. The medical records of 53 RP patients and 46 controls were reviewed. The OCTA images were obtained with the Cirrus 5000 with Angioplex, and an automated program was used to analyze the microvascular patterns. The perfusion density (PD) and vessel length density (VLD) were used as indices of the microvascular density, whereas the vessel diameter index (VDI) was used as a measure of the caliber of the vessels. The width of the ellipsoid zone (EZ) in the OCT images and the mean deviation (MD) of the Humphry Field Analyzer (HFA) were used to determine the severity of the RP. Student's *t*-tests and Spearman's correlation tests were used.

RESULTS. Both the PD and VLD in the superficial and deep plexuses and the whole retina were significantly reduced, and the VDI was significantly increased in RP patients compared with the corresponding values of the controls ($P < 0.001$). Spearman's rank tests indicated the RP severity was significantly correlated with the PD and VLD in all three layers ($P < 0.001$, r ranging from 0.50 to 0.87) and significantly correlated with VDI in the deep and the whole retina ($P < 0.001$, ranging from -0.64 to -0.73).

CONCLUSIONS. Quantitative changes in the microvascular density might be useful for examining the pathophysiology of RP.

Keywords: retinitis pigmentosa, optical coherence tomography angiography, quantitative analysis, perfusion density, vessel morphology

RP is a genetically heterogeneous group of inherited retinal disorders with degeneration of the rod and cone photoreceptors. The symptoms and signs of RP are impaired night vision; slow, progressive peripheral-to-central visual field loss; and a reduction of the visual acuity in the end stage. The attenuation of retinal vessels is a classic feature of RP in addition to atrophy of the RPE and peripheral bone spicule pigmentation. An impaired retinal flow has been suggested to be the underlying pathology of RP as determined by the findings made by multiple instruments.^{1–5} Most of these studies reported a decrease in the retinal blood flow in RP patients.

Optical coherence tomography angiography (OCTA) is a recent advance in the field of OCT, and its use enables clinicians to view the retinal vascular networks without the need for contrasting dyes. Usually, OCTA devices offer automated segmentation of the full-thickness retinal scans into several layers of the retina, such as superficial retinal vascular plexus, deep retinal vascular plexus, and choriocapillaris.

Several groups have recently reported abnormalities in the OCTA images in the eyes of RP patients, indicating a reduction of the retinal blood flow and an increase in the size of the foveal avascular zone (FAZ).^{6–10} In addition, some studies have reported significant correlations between the parameters of

the OCTA images and other functional and structural data, for example, visual acuity,^{8,9} visual fields,⁹ multifocal electroretinograms, and OCT parameter values.⁷ These results suggested that the microvasculature was more impaired in eyes with more severe retinal degeneration, that is, more advanced RP. However, some of the results were inconsistent with these findings, and the differences in the results may be due to differences of the genetic heterogeneity of the RP patients tested, the inclusion criteria, and the method of analyses. In addition, the evaluation of the average vascular density of the macula of RP has been the parameter mainly examined. However, the precise structural assessments of the blood vessel, such as whether the vessel diameter becomes thicker or thinner and whether the length of the blood vessel becomes longer or shorter, have not been examined by using these OCTA parameters.

Thus, the purpose of this study was to determine in detail the morphology of the microvasculature in eyes of patients with RP. To accomplish this, we used the Cirrus 5000 with Angioplex OCTA to obtain en face images of the superficial plexus, deep plexus, and the whole retina of 53 eyes of RP patients.¹¹ The OCTA images were analyzed with the Angio Exerciser software (Carl Zeiss Meditec, Inc., Dublin, CA, USA), which quantified the microvascular changes of not only the



vascular density but also the indices of vascular thickness and length. In addition, we examined whether the correlations between the microvascular indices and the retinal function and structure, including the best-corrected visual acuity (BCVA), automated static perimetry findings, and OCT findings, were significant.

METHODS

This was a retrospective study. All of the procedures conformed to the tenets of the Declaration of Helsinki, and the Institutional Review Board/Ethics Committee of the Nagoya University Graduate School of Medicine approved this study (no. 0538). An oral informed consent was obtained from the patients after an explanation of the procedures and purpose of the examinations.

Subjects

We reviewed the medical records of 282 RP patients who were examined at the Nagoya University Hospital. The diagnosis of RP was based on the presence of night blindness; peripheral visual field loss; typical fundus appearance, including changes of the RPE; blood vessel attenuation, bone spicule pigmentation, and a reduced ($<50 \mu\text{V}$) or extinguished full-field scotopic flash electroretinograms. From the 282 patients, we identified 71 patients who had undergone OCTA by Cirrus 5000 with Angioplex. Any images with significant artifacts due to blockage of the OCT signal by floaters, eyelashes, or movements were excluded. In addition, any images with significant segmentation errors as a result of pathologic changes, such as an epiretinal membrane, macular edema, or thinning of the retina, were also excluded.

In the end, 53 eyes of 53 RP patients (26 men and 27 women) were studied. Forty-six controls (25 men and 21 women) without any ocular or systemic disease were evaluated. The average (\pm standard deviation) age was 48.3 ± 17.3 years (range, 16–76 years) for the RP patients, and 52.7 ± 15.4 years (range, 20–75 years) for the controls. For the analyses, we selected eyes that had better-quality OCTA images, and if both eyes had similar quality of OCTA images, the right eyes were chosen. The first and the second authors (DI and SU) independently excluded the patients, and when there was a disagreement, the third author (TK) made the final decision.

All of the patients had undergone a complete ophthalmologic examination that included the measurements of the BCVA, spectral-domain OCT (SD-OCT), and perimetry with the Humphrey Field Analyzer (HFA; Carl Zeiss Meditec, Inc.). The mean deviation (MD) value of HFA 10-2 of the Swedish Interactive Threshold Algorithm program was used for the statistical analyses.

Analysis of SD-OCT

Cross-sectional images were obtained by radial scanning of 30 degrees with the SD-OCT instrument (Spectralis; Heidelberg Engineering, Heidelberg, Germany). All images were the average of 100 SD-OCT scans using the eye-tracking system. Only the horizontal and vertical scans centered on the fovea were evaluated. The ellipsoid zone (EZ) width was measured between the borders where the EZ band met the upper surface of the RPE using the built-in caliper. If the EZ width exceeded the scanned images, the border of the EZ was set as the edge of the scanned image. The average of the EZ width of the

horizontal and vertical images was used for the statistical analyses.^{12,13}

Analysis of OCTA Images

OCTA was performed with the Zeiss Cirrus 5000 with Angioplex (Carl Zeiss Meditec, Inc.). The Angioplex uses optical microangiography, a recently developed imaging technique that produces 3D images of the dynamic blood flow within the microcirculatory tissue beds.^{11,14} A scanned area of 3×3 mm centered on the fovea was used. All acquisitions were performed using the FastTrac retinal-tracking technology (Carl Zeiss Meditec, Inc.) to reduce motion artifacts. The segmentation of the retinal layers was automatically performed by the embedded software. In addition to the nonsegmented en face images (whole retina), en face images of the superficial retinal capillary layer (SRL) plexus and the deep retinal capillary layer (DRL) plexus were analyzed. We used SD-OCTA systems operating at 840 nm even though light at this wavelength is greatly scattered and absorbed by the RPE complex, which can affect the ability to examine the choriocapillaris vessels.^{15,16} We did not analyze the choriocapillaris vessels in this study. In addition, the clarity of the images of the choroidal vascular layer was dependent on the status of the RPE, which was affected by the stage of RP.⁸

In addition to the original images, binarized images and skeletonized images were obtained by the Angio Exerciser software, which was provided by Zeiss for research purposes only. The perfusion density (PD) was calculated as the percentage of the area occupied by vessels in the designated 3×3 -mm area based on the binarized images. After skeletonization of the binarized images, the vessel length density (VLD) was calculated as the percentage of area occupied by vessel in the designated 3×3 -mm area, and the VLD represents the vessel length per millimeter. The vessel diameter index (VDI) was calculated by dividing the value of PD by the VLD, which yields the average vessel caliber (in millimeters) in the SD-OCTA image.^{17,18} The VDI has been reported to have substantial potential in analyzing the mechanisms involved in retinal vascular diseases such as diabetic retinopathy, in which an increase in the VDI was significantly associated with a worsening of the disease.¹⁷

The FAZ area was measured using ImageJ software (<http://imagej.nih.gov/ij/>; provided in the public domain by National Institutes of Health, Bethesda, MD, USA) after setting the scale to 423×423 pixels in a 3×3 -mm² scanned area by one masked examiner (DI). The edge points were manually selected along the edge of the vessels. The area of the FAZ was calculated by multiplying the number of pixels within the contour by the area of a single pixel. The FAZ area was calculated only for the whole retina to reduce variations of the measurements.¹⁹

Statistical Analyses

Data are presented as the means \pm standard deviations. The decimal BCVA values were converted to logMAR for statistical analyses. Mann-Whitney *U* tests and *t*-tests were used to compare data sets as appropriate. Univariate analysis was performed with the Spearman's rank correlation coefficient tests. The significance of the correlations between the microvasculature values, the PD, VLD, VDI, and FAZ, were determined relative to the age, BCVA, EZ length, and the HFA10-2 MD values. A *P* value of <0.05 was considered statistically significant. When the Bonferroni correction was applied, the significance level was set at $\alpha = 0.0125$.

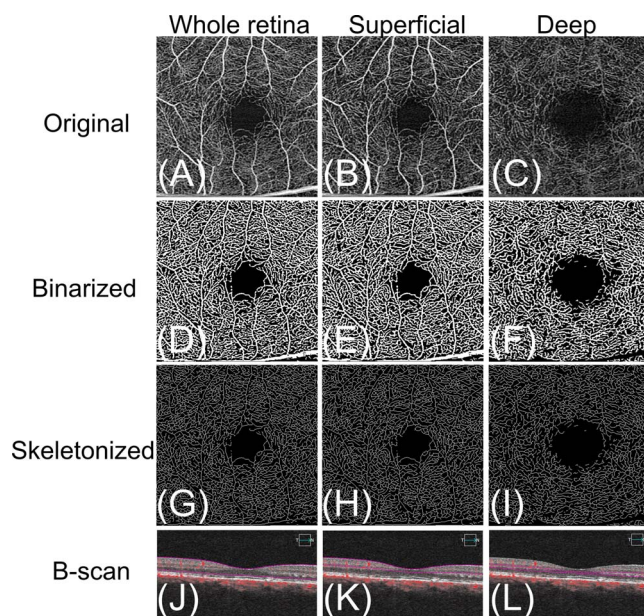


FIGURE 1. Representative segmented and nonsegmented OCTA images and their processed images of a control subject. Images of the nonsegmented whole retinal layer (A, D, G), segmented superficial retinal plexus (B, E, H), and segmented deep retinal plexus (C, F, I) in the right eye are shown. The original images (A–C), binarized images (D–F), and skeletonized images (G–I) are shown. The binarized images (D–F) and skeletonized images (G–I) were processed by Angio Exerciser software. The binarized images were obtained by binarization of original images and used for quantification of the PD. The skeletonized images were obtained by iteratively deleting the pixels in the outer boundary of the binarized image until one pixel remained in the width direction of the vessels. These images were used to estimate the VLD, which indicates the total length of the microvessels. All of the images are 3×3 mm. The B-scan images with segmentation (J–L) are shown. The B-scan images of the whole retina (J), superficial retinal plexus (K), and deep retinal plexus (L) are shown.

RESULTS

Representative OCTA Images of Control and RP Patients

Representative SD-OCTA images of a healthy control eye are shown in Figure 1. Three types of OCTA images (the original OCTA images, a binarized image, and a skeletonized image) of the whole retina and the superficial and deep layers are shown. The vessels detected in images of the whole retina and those of the superficial layer were quite similar.

The three types of OCTA images of three eyes with different severity of RP are shown in Figure 2. The original OCTA images, their binarized images, and skeletonized images of the superficial and deep layers are shown. The OCTA images of the whole retina are also shown in Supplementary Figure S1. The binarized or skeletonized images demonstrate the areas of vascular abnormalities more clearly than do the original OCTA images. In the eye with mild RP, the superficial and deep capillary plexuses appear to be barely affected. In the eye with more severe RP, the images show a greater reduction in the retinal vasculature. In general, capillaries of the deep layers were more altered than those of the superficial layer. The projection artifacts in the deep vascular layer, which are the fluctuating shadows cast by blood flowing in the superficial vascular layers,²⁰ were prominent in the images in the eyes of the more severe RPs, especially in binarized images. On the

other hand, in the eyes of the control subjects, the projection artifacts were less severe than those of the RP patients.

Analysis of Differences in OCTA Indices Between RP and Control Group

The demographic data of the 53 eyes of the 53 RP patients and 46 normal control eyes are summarized in Table 1. There were no significant differences in the sex distribution and age between RP and control group. The visual acuity was significantly lower in the RP group. The EZ was intact in the control eyes but disrupted in the RP eyes, except in one patient. The mean deviation of the HVA10-2 program was -16.03 dB for the RP patients. There were significant differences in the PD, VLD, and VDI of the superficial, deep, and whole retina between the eyes of the control and eyes of the RP patients ($P < 0.001$; Table 2). In addition, the FAZ area was larger in the RP group ($P < 0.001$). The VDI index in both the superficial and deep retinal levels was larger in the RP group. The significant negative correlation between the VLD and VDI indicated that the VDI increased as the VLD decreased in the analyzed three layers (Supplementary Fig. S2).

Correlation Between OCTA Indices and Other Clinical Functional or Structural Data

The correlations between the OCTA parameters and other parameters, including age, BCVA, EZ width, and MD of HFA10-2, are listed in Table 3. Age was not significantly correlated with any of the OCTA indices. The PD and VLD of the superficial and deep plexuses and the whole retina were significantly and negatively correlated with the BCVA and significantly and positively correlated with the MD of HFA10-2 and the EZ width. The VDI of the deep layer plexus and whole retina was significantly and positively correlated with the BCVA and significantly and negatively correlated with the MD of HFA10-2 and the EZ width. The results were comparable to the findings of the OCTA images, which showed less retinal vasculature in eyes with more severe RP (Fig. 2).

On the other hand, the size of the FAZ area was significantly correlated with the BCVA. These findings indicate that the PD and VLD represent the status of the progression of RP, and the size of the FAZ is related to the central macular function.

DISCUSSION

It has been reported that there is a reduction of retinal blood flow in the eyes of patients with RP as determined by different types of OCTA instruments, and our results are in general agreement. The values of the different OCTA parameters were significantly correlated with the severity of the RP determined by HVA findings and the EZ width.

One strength of our study was that information of the capillary plexuses, including the quantitative parameters of the PD, VLD, and VDI, was obtained. The results of the PD, which was quantified based on binarized images, and the VLD, which was based on the skeletonized images, had similar tendencies in the RP eyes. VDI has been reported to have substantial potential in analyzing the mechanisms involved in retinal vascular diseases, such as in diabetic retinopathy, that showed that the increase in the VDI was associated with a worsening of the disease.¹⁷

In the pathology of eyes with RP, a reduction of the oxygen consumption due to photoreceptor cell loss has been suggested to cause oxygen diffusion from the choroidal vessels into the inner retina, which decreased the need for oxygen delivery from the retinal circulation.^{21,22} This change of

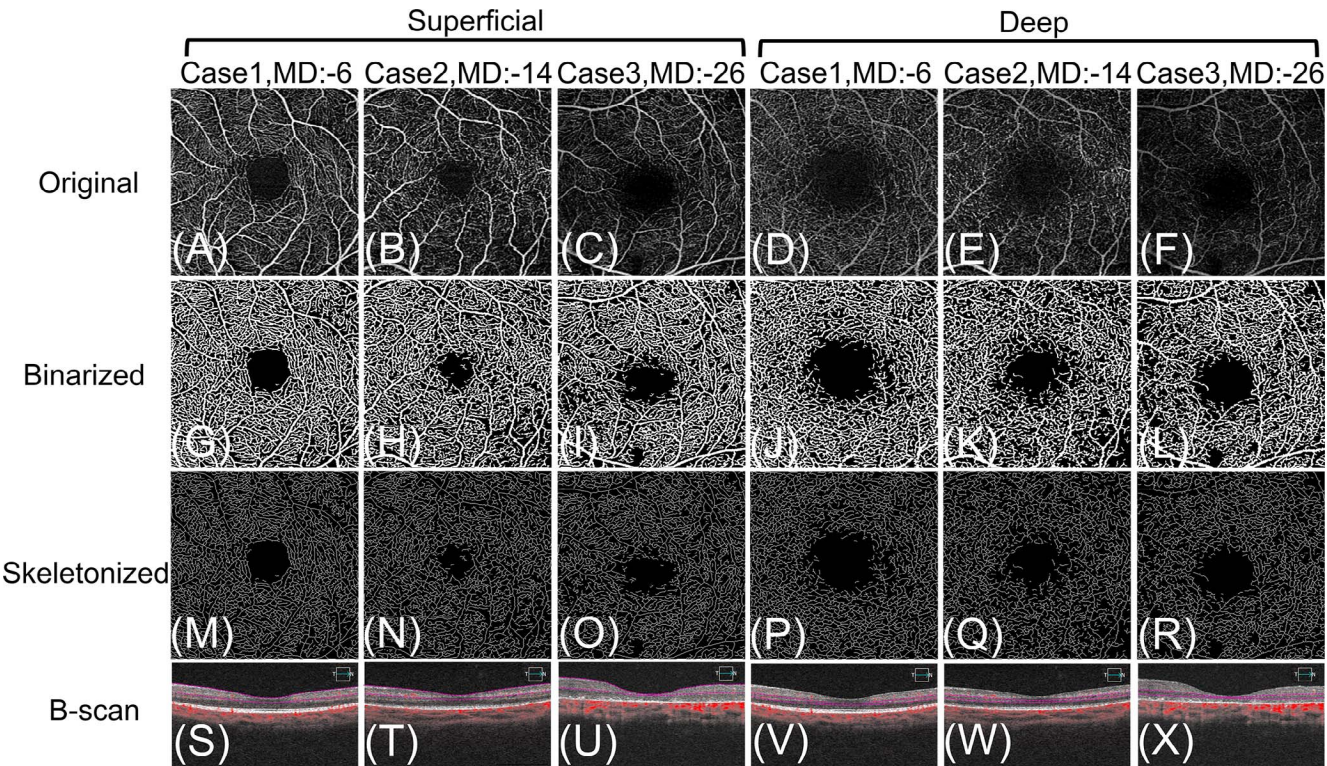


FIGURE 2. Representative OCTA images of the eyes of RP patients. The images of mild (A, D, G, J, M, P, S, V), moderate (B, E, H, K, N, Q, T, W), and severe (C, F, I, L, O, R, U, X) RP patients classified by the MD of the HFA are shown. Images of the segmented superficial retinal plexus (A–C, G–I, M–O, S–U) and the segmented deep retinal plexus (D–F, J–L, P–R, V–X) are shown. Original images (A–F), binarized images (G–L), and skeletonized images (M–R) are shown. The B-scan images (S–X) with segmentation are shown. The OCTA images show less retinal microvasculature in the more severe RP patients. The binarized and skeletonized images demonstrate the areas of vascular abnormalities more clearly than do the original OCTA images. The projection artifacts in the deep vascular plexus are prominent in the severe RP eyes.

oxygen diffusion was assumed to cause an attenuation of the vessels, but the change of the caliber of the retinal capillary was not determined. We had expected the reduction of the caliber of the capillary vessels in the eyes of the RP patients, but the results were the reverse. The VDI increased with increasing severity of the RP (Fig. 2) and with a decrease in the PD (Supplementary Fig. S2). There are two possible reasons for

the increased VDI; one is a real widening of the retinal capillaries, and the other is a larger contribution of larger vessel diameters due to loss of capillary flow. Because a greater increase in the dropout of the capillaries in eyes with more severe RP was seen in the OCTA images, we suggest that the latter was more influential. However, we need to consider the limitation of OCTA images: the signal void area in OCTA does not always mean vascular flow is lost, but it might indicate reduced blood flow below a certain threshold of OCTA detection.

There are several artifacts in OCTA imaging that might have blocked the mild microvascular changes in the RP eyes. First, poor fixation due to low visual acuity can cause motion artifacts that reduce the quality of the images. Second, projection artifacts were present, and although some investigators have attempted to develop algorithms to remove these artifacts,²³ there is no ideal way to address this problem. Analysis of the deep retinal plexus in RP eyes has been reported to be easily affected by projection artifacts,⁹ and our study was also affected by projection artifacts in eyes with RP. Although, Koyanagi et al.⁹ reported that the exclusion of projection artifacts did not affect the data, these artifacts may reduce image quality and accuracy of the deep retinal plexus to an unknown degree. Third, the automated segmentation algorithms used did not appear to be appropriate for some RP eyes, probably because of alterations of retinal morphology. We excluded 13 patients owing to obvious segmentation error, and these patients had relatively advanced visual field defects, for example, MD < –20 dB. This indicated that 43% of the RP patients who had MD worse than –20 dB were excluded.

TABLE 1. Demographic and Clinical Characteristics of Patients and Controls

Characteristic	Control Group	RP Group	P Value
Number of eyes	46	53	
Sex, males/females	25/21	26/27	
Age, y	52.7 ± 15.4	48.3 ± 17.3	0.32*
Visual acuity, logMAR	–0.001 ± 0.018	0.200 ± 0.257	<0.001†
EZ length, μm	8621.08 ± 426.18	2498.96 ± 1826.69	<0.001†
MD, dB		–16.03 ± 8.72	
Inheritance mode, n			
AD		7	
AR		6	
X-linked		0	
Sporadic		40	

Data are the means ± standard deviations. The P values are bold when they are less than or equal to the significance level cutoff of 0.05. AD, autosomal dominant; AR, autosomal recessive.

* t-tests.

† Mann-Whitney U tests.

TABLE 2. Indices of OCTA of Patients and Controls

Parameter	Control Group	RP Group	P Value
WPD	0.3895 ± 0.0204	0.3257 ± 0.0462	<0.001*
SPD	0.4166 ± 0.0080	0.3854 ± 0.0166	<0.001*
DPD	0.3475 ± 0.0298	0.2929 ± 0.0476	<0.001*
WVLD, mm ⁻¹	22.034 ± 1.371	17.566 ± 2.938	<0.001†
SVLD, mm ⁻¹	22.646 ± 0.755	20.204 ± 1.170	<0.001†
DVLD, mm ⁻¹	18.448 ± 1.769	14.766 ± 2.711	<0.001†
WVDI, mm	0.0176 ± 0.0004	0.0186 ± 0.0006	<0.001*
SVDI, mm	0.0184 ± 0.0003	0.0190 ± 0.0004	<0.001*
DVDI, mm	0.0188 ± 0.0004	0.0199 ± 0.0005	<0.001*
FAZ, mm ²	0.2310 ± 0.065	0.3091 ± 0.091	<0.001*

Data are the means ± standard deviations. The *P* values are bold when they are less than or equal to the significance level cutoff of 0.05. WPD, whole retinal perfusion density; SPD, perfusion density at the superficial retina plexus; DPD, perfusion density of the deep retina plexus; WVLD, whole retinal vessel length density; SVLD, vessel length density of the superficial retina plexus; DVLD, vessel length density of the deep retina plexus; WVDI, whole retinal vessel diameter index; SVDI, superficial vessel diameter index; DVDI, deep vessel diameter index.

* *t*-tests.

† Mann-Whitney *U* tests.

TABLE 3. Spearman's Correlation Coefficients Between OCTA Parameters and Other Parameters

Parameter	Age	Visual Acuity, logMAR	EZ Length	MD
WPD				
<i>P</i>	0.76	<0.001	<0.001	<0.001
<i>rs</i>	−0.04	−0.58	0.71	0.62
SPD				
<i>P</i>	0.94	<0.001	<0.001	<0.001
<i>rs</i>	0.01	−0.68	0.87	0.70
DPD				
<i>P</i>	0.05	0.001	<0.001	<0.001
<i>rs</i>	−0.26	−0.43	0.50	0.50
WVLD				
<i>P</i>	0.95	<0.001	<0.001	<0.001
<i>rs</i>	−0.01	−0.60	0.74	0.64
SVLD				
<i>P</i>	0.66	<0.001	<0.001	<0.001
<i>rs</i>	0.05	−0.45	0.79	0.65
DVLD				
<i>P</i>	0.13	<0.01	<0.001	<0.001
<i>rs</i>	−0.21	−0.45	0.55	0.54
WVDI				
<i>P</i>	0.56	<0.001	<0.001	<0.001
<i>rs</i>	−0.07	0.62	−0.73	−0.70
SVDI				
<i>P</i>	0.49	0.65	0.02	0.08
<i>rs</i>	−0.09	0.06	−0.30	−0.23
DVDI				
<i>P</i>	0.93	<0.001	<0.001	<0.001
<i>rs</i>	−0.01	0.46	−0.64	−0.64
FAZ				
<i>P</i>	0.92	<0.01	<0.01	0.02
<i>rs</i>	−0.01	0.39	−0.34	−0.30

Univariate analysis: Spearman's rank correlation coefficients (*rs*). Bonferroni correction was applied; the significance level was set at $\alpha = 0.0125$. The *P* values are bold when they are less than or equal to the significance level cutoff of 0.0125.

To minimize projection artifact and segmentation error, analysis of the whole retina without segmentation was also performed. The values of the OCTA parameters of the whole retina in RP eyes had tendencies similar to those from the superficial and deep vascular plexuses. Analysis of the whole retina would be another choice to analyze RP eyes to avoid the artifacts.

There are several limitations in our study. One is the lack of genetic data, and the relationship between the causative gene variants and the microvascular structures could not be determined. Second, the evaluated area was very small and restricted. The area damaged in RP is dependent on the stage, and because we analyzed only a 3×3 -mm area, we could not find many abnormalities in the early stage of RP. Analysis of a larger area with advanced instruments should be informative. Mastropasqua et al.²⁴ have reported a reduction in the density of the radial peripapillary capillary network vessels in eyes affected by RP, and this type of analyses might be another option for analyzing the microvessels in the eyes of RP patients.

In conclusion, our results show that both qualitative and quantitative changes in the microvascular density and morphology are useful in assessing the pathophysiology of RP. However, we need to pay careful attention when analyzing the deep capillary plexus because of projection artifacts. In addition, our findings suggest that these microvascular parameters can be markers for the progression of retinal diseases.

Acknowledgments

The authors thank Emerituc Duco Hamasaki, PhD (Bascom Palmer Eye Institute), for discussions and for editing the final version of the manuscript.

Supported in part by the Japan Society for the Promotion of Science (JSPS) KAKENHI Grants 16K11320 (SU) and 16K11265 (YT) and a Takayanagi Retina Research Award (SU).

Disclosure: **D. Inooka**, None; **S. Ueno**, None; **T. Kominami**, None; **A. Sayo**, None; **S. Okado**, None; **Y. Ito**, None; **H. Terasaki**, None

References

- Krill AE, Archer D, Newell FW. Fluorescein angiography in retinitis pigmentosa. *Am J Ophthalmol*. 1970;69:826–835.
- Hyvarinen L, Maumenee AE, Kelley J, Cantollino S. Fluorescein angiographic findings in retinitis pigmentosa. *Am J Ophthalmol*. 1971;71:17–26.
- Grunwald JE, Maguire AM, Dupont J. Retinal hemodynamics in retinitis pigmentosa. *Am J Ophthalmol*. 1996;122:502–508.
- Zhang Y, Harrison JM, Nateras OSE, Chalfin S, Duong TQ. Decreased retinal-choroidal blood flow in retinitis pigmentosa as measured by MRI. *Doc Ophthalmol*. 2013;126:187–197.
- Murakami Y, Ikeda Y, Akiyama M, et al. Correlation between macular blood flow and central visual sensitivity in retinitis pigmentosa. *Acta Ophthalmol*. 2015;93:E644–E648.
- Parodi MB, Cicinelli MV, Rabiolo A, et al. Vessel density analysis in patients with retinitis pigmentosa by means of optical coherence tomography angiography. *Br J Ophthalmol*. 2017;101:428–432.
- Toto L, Borrelli E, Mastropasqua R, et al. Macular features in retinitis pigmentosa: Correlations among ganglion cell complex thickness, capillary density, and macular function. *Invest Ophthalmol Vis Sci*. 2016;57:6360–6366.
- Sugahara M, Miyata M, Ishihara K, et al. Optical coherence tomography angiography to estimate retinal blood flow in eyes with retinitis pigmentosa. *Sci Rep*. 2017;7:46396.

9. Koyanagi Y, Murakami Y, Funatsu J, et al. Optical coherence tomography angiography of the macular microvasculature changes in retinitis pigmentosa [published online ahead of print 5 2017]. *Acta Ophthalmol*. doi:10.1111/aos13475.
10. Rezaei KA, Zhang QQ, Chen CL, Chao JF, Wang RK. Retinal and choroidal vascular features in patients with retinitis pigmentosa imaged by OCT based microangiography. *Graefes Arch Clin Exp Ophthalmol*. 2017;255:1287-1295.
11. Rosenfeld PJ, Durbin MK, Roisman L, et al. Zeiss Angioplex™ spectral domain optical coherence tomography angiography: technical aspects. In: Bandello F, Souied EH, Querques G, eds. *OCT Angiography in Retinal and Macular Diseases*. Basel: Karger; 2016;56:18-29.
12. Kominami A, Ueno S, Kominami T, et al. Restoration of cone interdigitation zone associated with improvement of focal macular ERG after fovea-off rhegmatogenous retinal reattachment. *Invest Ophthalmol Vis Sci*. 2016;57:1604-1611.
13. Kominami T, Ueno S, Kominami A, et al. Associations between outer retinal structures and focal macular electroretinograms in patients with retinitis pigmentosa. *Invest Ophthalmol Vis Sci*. 2017;58:5122-5128.
14. Wang RK, Jacques SL, Ma Z, Hurst S, Hanson SR, Gruber A. Three dimensional optical angiography. *Opt Express*. 2007;15:4083-4097.
15. Miller AR, Roisman L, Zhang Q, et al. Comparison between spectral domain and swept source optical coherence tomography angiographic imaging of choroidal neovascularization. *Invest Ophthalmol Vis Sci*. 2017;58:1499-1505.
16. Zhang Q, Chen CL, Chu Z, et al. Automated quantitation of choroidal neovascularization: a comparison study between spectral domain and swept source OCT angiograms. *Invest Ophthalmol Vis Sci*. 2017;58:1506-1513.
17. Kim AY, Chu ZD, Shahidzadeh A, Wang RKK, Puliafito CA, Kashani AH. Quantifying microvascular density and morphology in diabetic retinopathy using spectral-domain optical coherence tomography angiography. *Invest Ophthalmol Vis Sci*. 2016;57:OCT362-OCT370.
18. Chu Z, Lin J, Gao C, et al. Quantitative assessment of the retinal microvasculature using OCT angiography. *J Biomed Opt*. 2016;21:066008.
19. Coscas F, Sellam A, Glacet-Bernard A, et al. Normative data for vascular density in superficial and deep capillary plexuses of healthy adults assessed by optical coherence tomography angiography. *Invest Ophthalmol Vis Sci*. 2016;57:OCT211-OCT223.
20. Spaide RF, Fujimoto JG, Waheed NK. Image artifacts in optical coherence angiography. *Retina*. 2015;35:2163-2180.
21. Eysteinnsson T, Hardarson SH, Bragason D, Stefansson E. Retinal vessel oxygen saturation and vessel diameter in retinitis pigmentosa. *Acta Ophthalmol*. 2014;92:449-453.
22. Turksever C, Valmaggia C, Orgul S, Schorderet DF, Flammer J, Todorova MG. Retinal vessel oxygen saturation and its correlation with structural changes in retinitis pigmentosa. *Acta Ophthalmol*. 2014;92:454-460.
23. Zhang A, Zhang Q, Wang RK. Minimizing projection artifacts for accurate presentation of choroidal neovascularization in OCT micro-angiography. *Biomed Opt Express*. 2015;6:4130-4143.
24. Mastropasqua R, Borrelli E, Agnifili L, et al. Radial peripapillary capillary network in patients with retinitis pigmentosa: an optical coherence tomography angiography study. *Front Neurol*. 2017;27:572.